Forced convection rheoforming process for preparation of 7075 aluminum alloy semisolid slurry and its numerical simulation

Bing ZHOU[1], Yong-lin KANG[1,2], Guo-ming ZHU[1], Jun-zhen GAO[1], Ming-fan QI[1], Huan-huan ZHANG[1]

1. School of Materials Science and Engineering, University of Science and Technology Beijing, Beijing 100083, China;
2. State Key Laboratory for Advanced Metals and Materials, University of Science and Technology Beijing, Beijing 100083, China

Abstract: A self-developed forced convection rheoforming (FCR) machine for the preparation of light alloy semisolid slurry was introduced. The microstructure characteristics of 7075 aluminium alloy semisolid slurry at different stirring speeds prepared by the FCR process were analyzed. The experimental results suggest that with the increase of the stirring speed, the mean grain size of the semisolid decreases and the shape factor as well as the number of primary grains increase. Meanwhile, the preparation process of semisolid slurry was numerically simulated. The flow characteristics of the melt in the device and the effect of the stirring speed on temperature field and solid fraction of the melt were investigated. The simulated results show that during the preparation process of semisolid slurry, there is a complex convection within the FCR device that obviously changes the temperature field distribution and solid fraction of the melt. When the convection intensity increases, the scope of the undercooling gradient of the melt is reduced and temperature distribution is improved.

Key words: 7075 aluminum alloy; forced convection rheoforming (FCR); semisolid slurry; preparation; numerical simulation

1 Introduction

7075 wrought aluminum alloy has many good properties such as high strength, high hardness and light mass. It is widely used in aerospace and automotive field [1,2]. Reducing cost is a primary reason to consider the use of casting. This is usually achieved by replacing assemblies of numerous detailed parts or by replacing the parts that require complex machining and fabrication operations. However, the conventional casting process has disadvantages in casting such as pore defects, which lead to lower strength and limit the development and application of high performance aluminium alloy [3−5]. However, an alternative semisolid metal (SSM) process was developed in 1971 [6]. The SSM process combines the advantages of plastic processing and solidification processing. It can make complicated-structure products within one-step forming while refining the crystal structure and reducing defects like hot tears or solidification shrinkage [7−11].

After years of research and practice, process issues still exist in thixoforming such as complex process, high energy consumption, inefficiency and high-cost. Hence, the focus of current studies of SSM process has turned back to the rheoforming research in recent years [12−16]. One of the main research directions of rheoforming process is developing the efficient and reliable equipments and techniques for the preparation of semisolid slurry. So far, many semisolid slurry preparation technologies and forming processes have been proposed such as two-screw rheoforming process (TSR) [17], low superheat pouring with a shear field process (LSPSF) [18], serpentine channel pouring process (SCP) [19], gas induced semisolid process (GISS) [20], continuous rheoconversion process (CRP) [21] and taper barrel rheoforming process (TBR) [22].

A self-developed forced convection rheoforming (FCR) machine was designed for the preparation of light alloy semisolid slurry by KANG et al [23]. It is high efficient, reliable and easy to maintain. It can work all day without clean-up. The stable semisolid slurry with homogeneous and fine microstructure could be obtained by the FCR process. Furthermore, it is convenient to

combine FCR device with traditional metal forming processes to develop new rheoforming process.

Stirring speed is one of the major factors that affect microstructure in the FCR process. Taking 7075 aluminium alloy as experimental material, the microstructure characteristics and microstructure evolution of the SSM slurry at different stirring speeds were analyzed in this work. Based on heat transfer and hydrodynamics, the flow characteristics and the effect of stirring speed on the distribution of temperature field and solid fraction were investigated with the reliable commercial CFD software Flow-3D.

2 Experimental procedures and numerical simulation

2.1 FCR device

Figure 1 illustrates the structure of FCR machine. The machine consists of a shearing system, a temperature control system and an emptying system, with the advantages of high efficient, reliable and easy to maintain. The shearing system includes the spiral rod equipped with helical blade and mixing chamber with graphite sleeve. The temperature control system contains heating and cooling elements on the wall of the stainless barrel to ensure a constant temperature. The emptying process is achieved through emptying handle connected with graphite blockage. When the SSM slurry is prepared, the graphite blockage blocks the slurry outlet to avoid the leakage of the alloy melt under the action of the strong spring. After SSM slurry being prepared, the SSM slurry flows out by turning round emptying handle and raising
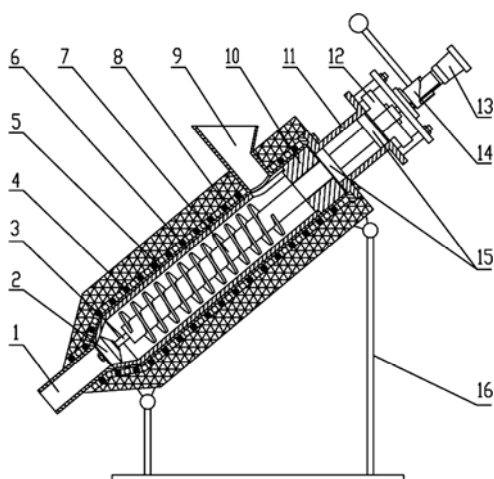

Fig. 1 Schematic diagram of integrated FCR machine: 1—Slurry outlet; 2—Graphite blockage; 3—Emptying core bar; 4—Heating and cooling elements; 5—Stainless barrel; 6—Graphite inner sleeve; 7—Spiral stirring rod; 8—Insulation; 9—Funnel; 10—Graphite insulation ring; 11—Bearing block; 12—Gear; 13—Adjusting handle; 14—Emptying handle; 15—Bearing; 16—Adjustable bracket

the graphite blockage. 5 kg semisolid slurry can be prepared by the machine once according to its bulk. If a large amount of slurry is required once, it could be achieved through continuous pouring without blockage. The temperature control system can assure accurate stable barrel temperature through heating and cooling elements. The device can work continuously and steadily because the feed inlet, discharge port and mixing chamber are all equipped with graphite lining to minimize sticking material.

The operating principle of FCR machine is as follows: while stirring, the melt in the mixing chamber has complicated convection characteristics. In the meantime, under the cooling effect of the device, the generation environment for dendrites has been destroyed and the grains incline to grow up as nearly spherical. The main factors affecting the preparation of semisolid slurry are pouring temperature, barrel temperature, stirring speed and mixing time.

2.2 Experimental material and procedures

The experimental material is commercial 7075 high strength aluminium alloy with the chemical composition given in Table 1. The solidus and liquids were determined by differential scanning calorimetry (DSC). The samples of about 3 mm in diameter and 1 mm in height were cut, sandpapered, and then put into carbon pans with lids in argon atmosphere. The samples were heated to 700 °C at 5 °C/min and cooled to room temperature at the same rate. The studied alloy has a melting range of 477−640 °C.

Table 1 Chemical composition of 7075 aluminium alloy ingot (mass fraction, %)

Zn	Mg	Cu	Cr	Mn	Fe	Al
5.80	2.41	1.62	0.23	0.01	0.20	Bal.

For SSM processing, the FCR process is shown in Fig. 2. The aluminium alloy ingot was dried and then put into a melting furnace. After refinement and degassing treatment at 710 °C, liquid alloy was set aside for about 15 min and cooled to the pouring temperature (0−30 °C above the liquidus). About 2 kg of the alloy was poured into the FCR machine at 640 °C. The graphite inner sleeve was controlled at temperature of 620−580 °C, stirring speed of 100−500 r/min and stirring time of 10−90 s. The liquid alloy in the device was influenced both by stirring and cooling effect. The prepared slurries were poured into a special stainless barrel and cooled in water.

The samples were ground, polished and etched by Keller reagent. The effects of process parameters on the primary α(Al) particle size and the shape factor were investigated. The shape factor (F) was calculated by

$F=4\pi A/P^2$. In this formula, A and P are respectively the total area and the peripheral length of the primary particles. Therefore, F is 1 for perfect spherical particles.
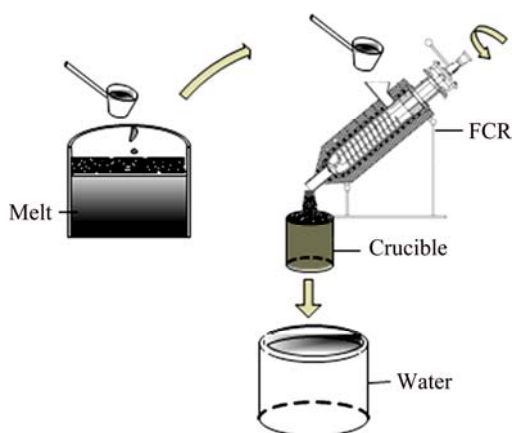

Fig. 2 Schematic diagram of FCR process

2.3 Simulation

The simulation procedures for exploring the fluid status in FCR device are as follows. Firstly, the 3D solid model was created by Pro/E CAD/CAM software. Secondly, the standard joint form IGES or STL file was output. Thirdly, the above model was transmitted to meshing-geometry block in Flow-3D software. Then, the pre-processing module set some parameters such as material data, heat exchange coefficient, initial temperature and convergence accuracy. After the calculation, simulation results were observed and analyzed directly through the post-processing block.

Knowing the changes of physical field in the FCR process is crucial to understanding the solidification of semisolid slurry and adjusting the FCR parameters to refine the microstructure. One of the key points is to explore the flow characteristics of the melt in FCR device and the effect of stirring speed on the preparation of semisolid. The flow behaviour of the melt in FCR process can be divided into pouring and stirring. The pouring time is short in entire FCR process, so, in this work, the stirring process was mostly focused on. Therefore, it assumes that the melt already exists in the device and it can be achieved by pre-loading the fluid into the model in Flow-3D software. The simplified model and generation mesh are shown in Fig. 3. After meshing the total number of elements is 160000. The width of the grid is 2.2 mm. Most of thermal properties of 7075 alloy come from thermodynamic database calculation in Procast software [24], which is basically consistent with experimental value. Figure 4 shows the contrast solid fractions of calculated data and experimental data.

The simulation of the effect of stirring speed on the preparation of semisolid slurry is an important aspect.
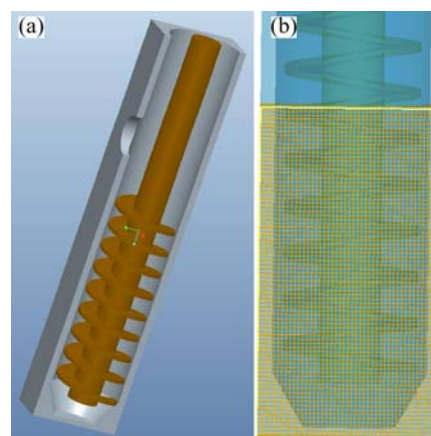

Fig. 3 Simplified 3D model (a) and generation mesh (b) of FCR device
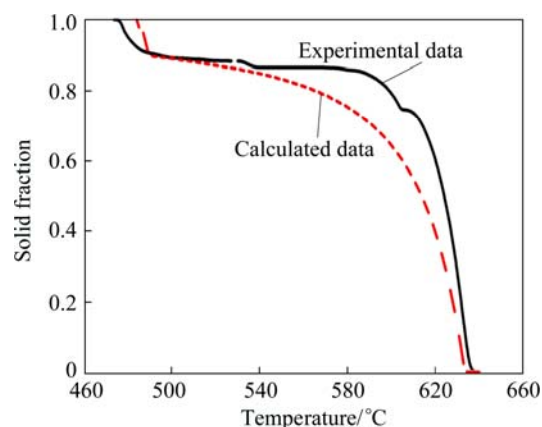

Fig. 4 Curves of solid fraction versus temperature by calculation and experiment

The stirring speeds of the experiments are 0−400 r/min and the corresponding angular velocities for the simulation are 0−25.12 rad/s according to adjustable speed motors. Table 2 lists several important parameters such as initial melt temperature, initial melt volume, initial barrel temperature and related parameters about heat transfer.

Table 2 Process and initial conditions of simulation

Input	Value
Initial melt temperature/°C	640
Initial melt volume/mL	500
Initial barrel temperature/°C	610
Initial agitating shaft temperature/°C	610
Thermal conductivity of graphite sleeve/(W·m^{-1}·K^{-1})	129
Thermal conductivity of agitating shaft/(W·m^{-1}·K^{-1})	23.4
Heat transfer to fluid/(kW·m^{-2}·K^{-1})	20

3 Results and discussion

3.1 Effect of stirring speed on microstructure of semisolid

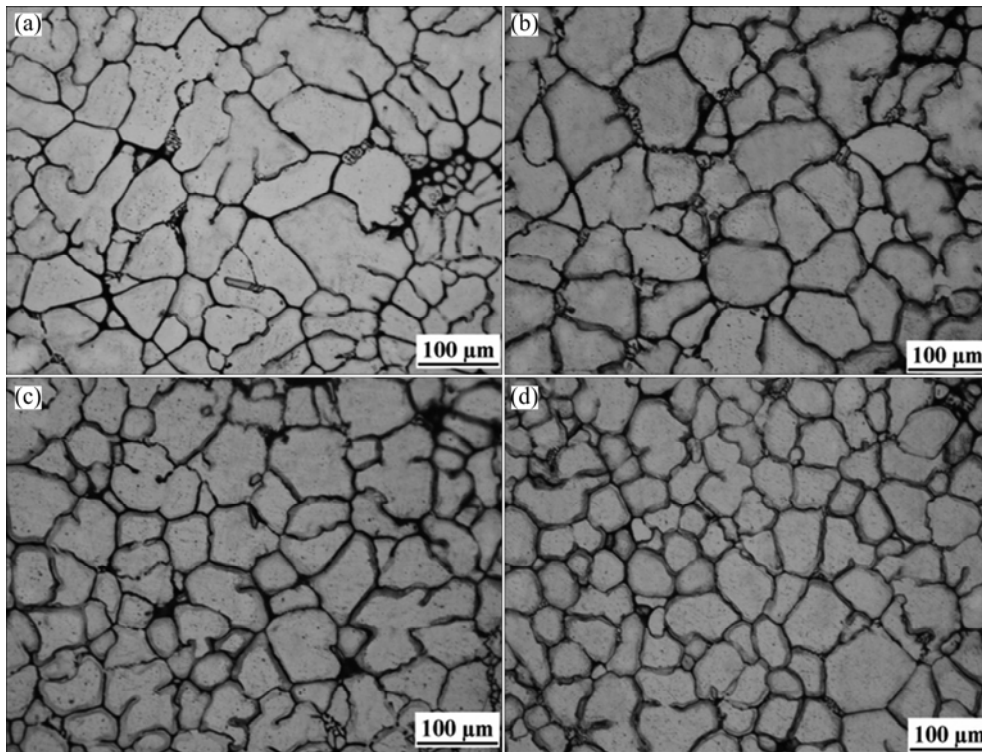Figure 5 shows the optical micrographs of semisolid

Fig. 5 Optical micrographs of semisolid 7075 aluminum alloy at different stirring speeds: (a) 100 r/min; (b) 200 r/min; (c) 300 r/min; (d) 400 r/min

7075 aluminium alloy at pouring temperature of 640 °C, barrel temperature of 610 °C and mixing time of 30 s and different stirring speeds. It reveals that all the microstructures of semisolid aluminium alloy by the FCR process are obviously different with the traditional casting microstructures. The microstructure mainly consists of rose and spherical primary α(Al) particles. When the stirring speed is 100 r/min, the microstructure includes rose-like particles and small dendrites, the mean size of primary particles is about 104 μm and the degree of globularity is about 0.6. With the increase of stirring speed, the number of dendrites decreases, the mean size of primary particles reduces and the shape factor increases. This development can be attributed to the increase of convection intensity. When the stirring speed is 400 r/min, the mean particle size is 77 μm and the shape factor is 0.76. The very little liquid-state microstructure shown in Fig. 5 is different from the curve of solid fraction versus temperature shown in Fig. 4. It can be explained that the liquid content in the micrographs is not the true quantity presented at related temperature. It is because the quenching process is not rapid enough to freeze the liquid content entirely and timely for high composition multiple aluminium alloy [25].

Figure 6 shows the mean size and the shape factor of primary particles at different stirring speeds. When the stirring speed is 100 r/min, the rotational rate of the melt
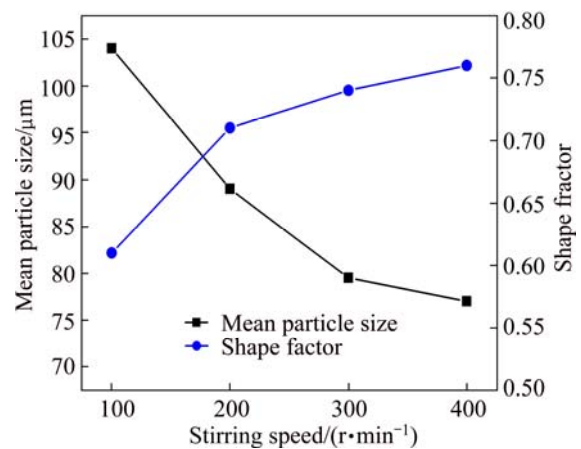

Fig. 6 Variation of mean size and shape factor of primary particles with stirring speed

is small and the convection intensity of the melt is relatively low. Large temperature difference exists in the melt, and due to weak convection, the melt needs a long time to reach the relatively uniform temperature distribution in FCR device. When the stirring speed increases, less time is needed to reach the uniform temperature distribution of the melt. The preferential growth of grains in a relatively uniform temperature field is inhibited due to small undercooling gradient. The grains grow uniformly in all directions. This is conductive to the growth of globular grains but not to the dendrites. Moreover, according to traditional crystal

dissociating theory [26], some grains adhered on the wall or helical blade to nucleate are easier to free to the melt under scouring action because of increasing convection intensity of the melt, so it can increase the grain quantity.

From Figs. 5 and 6, it can be summarized that, with the increase of stirring speed, the melt needs less time to reach the uniform temperature distribution in FCR device. The small undercooling gradient and the convection state are not conducive to the dendrite growth. The grains incline to grow up as nearly spherical. The semisolid slurry can be prepared with small homogenous primary particles by the FCR process.

3.2 Flow characteristics of melt in FCR device

Figure 7 illustrates the flow characteristics of the 7075 aluminium alloy melt inside the FCR device during the slurry preparation. After flowing into the FCR device, under the action of gravity and stirring rod equipped with helical blade, the melt flows from high to low along the graphite wall. At the bottom of the mixing chamber, the molten alloy has complex stirring-mixed flow characteristics. It can be divided into two parts: axial flow and circular flow. The prepared SSM slurry will flow out with the help of discharge procedure after setting periods of time.

Flow velocity was simulated to better understand the flow characteristic of the melt in the device. As shown in Fig. 8, the velocity vector of the fluid in three dimensional directions can be decomposed into the axial velocity vector and circular velocity vector in 2D pattern for flow analysis in FCR device. The condition was obtained by mixing 30 s at initial pouring temperature of 640 °C, initial barrel temperature of 610 °C and the stirring speed of 300 r/min. In Fig. 8(a), it is obvious that the axial velocity vector consists of two parts: internal
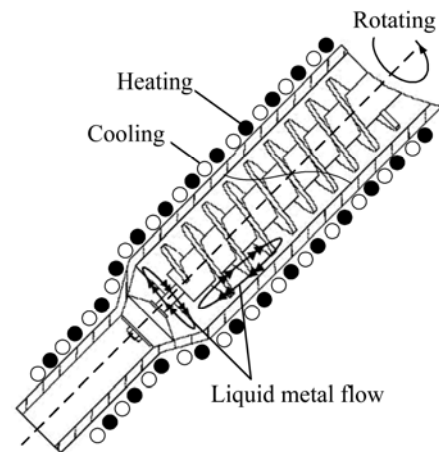

Fig. 7 Flow illustration of 7075 aluminum alloy melt in FCR device

axial velocity vector from high to low under the action of helical blade's compression and gap velocity vector from low to high due to the reaction of axial flow. The melt has a sufficient velocity field in axial direction except the bottom. At the bottom the weak convection might lead to inadequate heat transfer and the temperature is higher than that at other places. Meanwhile, the melt has the circular velocity vector in the same direction with stirring direction as shown in Fig. 8(b). The simulation result of flow characteristics in FCR device is consistent with the prediction in Fig. 7.

3.3 Simulation of stirring speed on temperature field

Understanding the changes of temperature field is crucial to studying the preparation process of slurry. The effect of stirring speed on temperature field and solid fraction was simulated for understanding FCR process and adjusting process parameters to guide the experiment. Figure 9 shows the simulated temperature field and solid
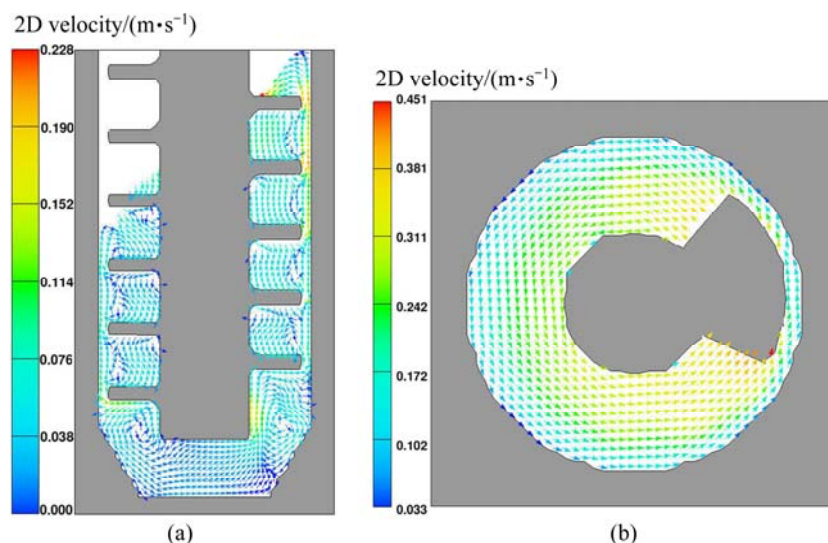

Fig. 8 Flow velocity field distribution of 7075 aluminum alloy melt in FCR device: (a) Axial velocity vector; (b) Circular velocity vector
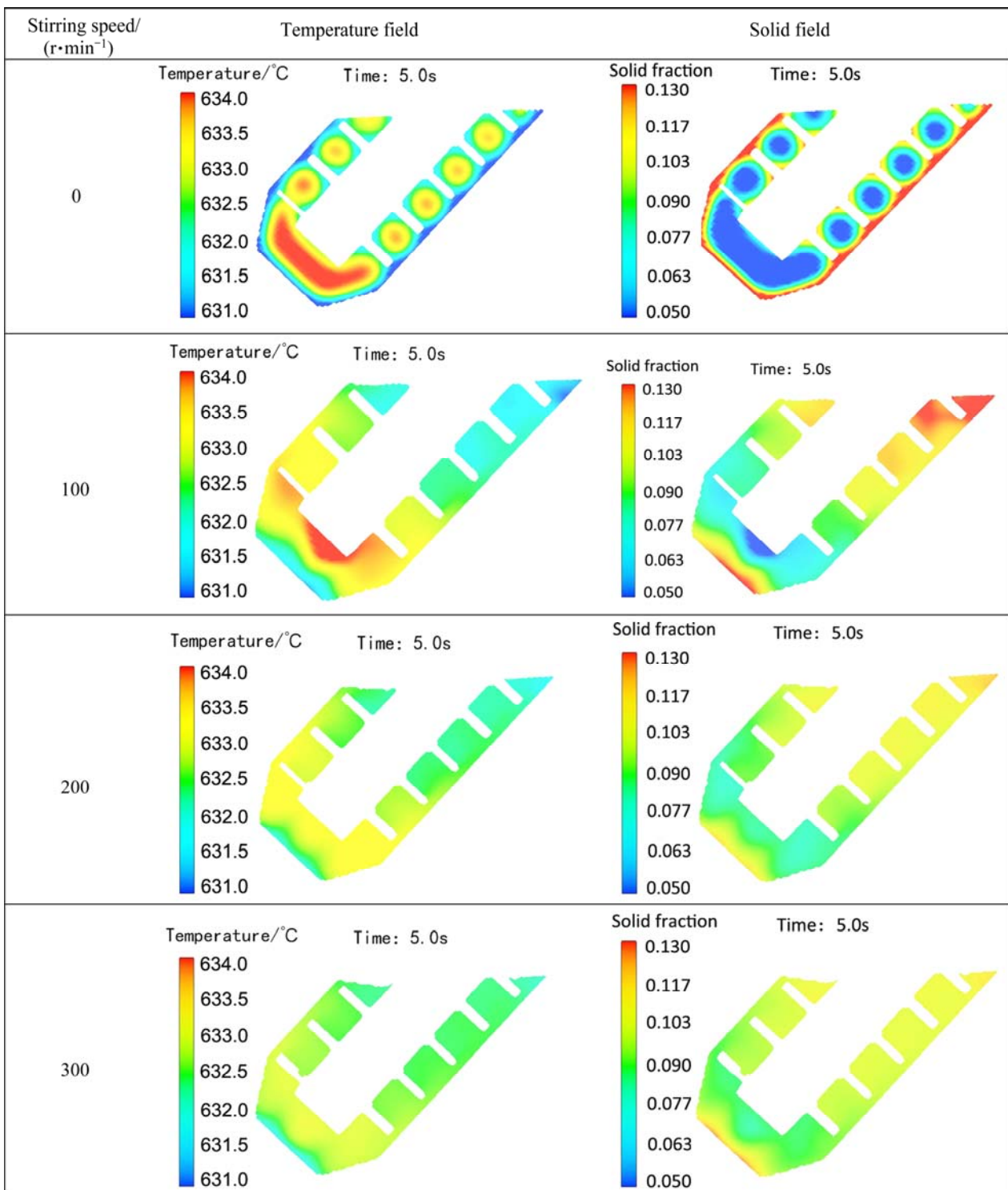
Fig. 9 Temperature field and solid fraction simulation versus stirring speed

fraction simulation versus stirring speed at simulation parameters shown in Table 2. When stirring speed is 0, the melt near the wall and helical blade cools down rapidly and the new grain forms quickly. But the rest of the melt cools slowly only by heat conduction within the melt and fewer grains form. The great temperature difference and uneven distribution of the primary particles are not good for semisolid slurry for dendrites.

When stirring speed is 100 r/min, the distributions of temperature field and solid fraction are changed greatly in comparison with those at stirring speed of 0. Even so, there is still a large temperature difference at the bottom. Because weak convection of the bottom leads to inadequate heat transfer as shown in Fig. 8(a), it needs more time to reduce temperature difference. When the stirring speed is 200 r/min, the temperature difference of

the melt is limited to 2 °C and the distribution of the primary particles is more even through increasing convection and the bottom condition is improved. When the stirring speed is 300 r/min, the temperature distribution throughout the melt is more homogeneous and the temperature difference of the melt is limited to 1 °C. The small undercooling gradient around the grains is beneficial to promoting the grains in quantity and morphology. The grains evenly distribute in the continuous convection melt, which effectively reduces the possibility that the grains grow into dendrites.

On the basis of simulation results, it can be considered that, when the temperature difference of the melt is within 1 °C and the melt is in a convection state, the dendrite formation environment will be destroyed. It is very conductive to the growth of spherical grains. If the special state is called balance state, the time before entering the state is called imbalance time. The variation of imbalance time with stirring speed is shown in Fig. 10. When the stirring speed is 100 r/min, the convection intensity of the melt is low and there is a large temperature difference inside the melt. The slurry needs more time to achieve the uniform temperature state. With the increase of the stirring speed, the temperature difference reduces fast, at the same time, the imbalance time significantly decreases because of the increase of convection intensity. It is very efficient to distribute temperature field uniformly. The shorter the imbalance time lasts, the less the dendrites or irregular grains generate. Therefore, increasing stirring speed is beneficial to reducing the size and modifying the morphology. These results are consistent with the experiment results shown in Fig. 5.
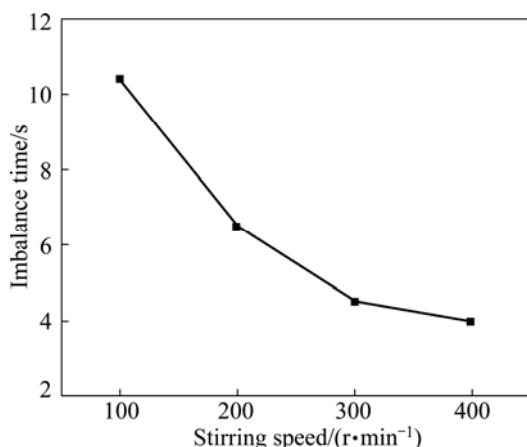

Fig. 10 Variation of imbalance time with stirring speed

4 Conclusions

1) An FCR machine was designed for the preparation of light alloy semisolid slurry. It consists of a shearing system, a temperature control system and an emptying system. It shows merits of high efficiency, reliability and handleability to maintain. The semisolid microstructure of the 7075 Al alloy with nearly spherical and uniformly distributed α(Al) small primary particles in the matrix can be obtained.

2) Increasing stirring speed can enhance the convection intensity of the melt. As the stirring speed increases, the primary α(Al) particles of semisolid slurry increase in quantity and become nearly spherical. When the stirring speed is 400 r/min, the mean particle size of semisolid microstructure is 77 μm and the shape factor is 0.76, while other corresponding processing parameters are the pouring temperature of 640 °C, the barrel temperature of 610 °C and the mixing time of 30 s.

3) The melt in the device has complex convection characteristics: the axial flow and circular flow. The temperature of the melt has uniform distribution because of the convection, which is obviously different from the traditional temperature distribution during the casting solidification process. As stirring speed increases, the temperature field can reach balance faster and the grain distribution is more even. The small undercooling gradient and the convection state of the melt can effectively destroy the dendrites generation environment and reduce the generation possibility of dendrites.

References

[1]   STARKE E A Jr, STALEY J T. Application of modern aluminium alloys to aircraft [J]. Progress in Aerospace Sciences, 1996, 32(2−3): 131−172.
[2]   WILLIAMS J C, STARKE E A Jr. Progress in structural materials for aerospace systems [J]. Acta Materialia 2003, 51(19): 5775−5799.
[3]   KIM S W, KIM D Y, KIM W G, WOO K D. The study on characteristics of heat treatment of the direct squeeze cast 7075 wrought Al alloy [J]. Materials Science and Engineering A, 2001, 304−306: 721−726.
[4]   THANABUMRUNGKUL S, JANUDOM S, BURAPA R, DULYAPRAPHANT P, WANNASIN J. Industrial development of gas induced semisolid process [J]. Transactions of Nonferrous Metals Society of China, 2010, 20(s): s1016−s1021.
[5]   MAHATHANINWONG N, PLOOKPHOL T, WANNASIN J, WISUTMETHANGOON S. T6 heat treatment of rheocasting 7075 Al alloy [J]. Materials Science and Engineering A, 2012, 532: 91−99.
[6]   SPENCER D B, MEHRABIAN R, FLEMINGS M C. Rheological behaviour of Sn-15 pct Pb in the crystallization range [J]. Metallurgical Transactions, 1972, 3(7): 1925−1932.
[7]   JI S, FAN Z, BEVIS M J. Semisolid processing of engineering alloys by a twin-screw rheomoulding process [J]. Materials Science and Engineering A, 2001, 299: 210−217.
[8]   JANUDOM S, RATTANOCHAIKUL T, BURAPA R, WISUTMETHANGOON S, WANNASIN J. Feasibility of semi-solid die casting of ACD12 aluminum alloy [J]. Transactions of

Nonferrous Metals Society of China, 2010, 20(9): 1756−1762.

[9]   SUYTINO, ESKIN D G, KATGERMAN L. Structure observations related to hot tearing of Al-Cu billets produced by direct-chill casting [J]. Materials Science and Engineering A, 2006, 420(1−2): 1−7.

[10] PHILLION A B, COCKCROFT S L, LEE P D. A new methodology for measurement of semisolid constitutive behaviour and its application of as-cast porosity and hot tearing in aluminium alloys [J]. Materials Science and Engineering A, 2008, 491(1−2): 237−247.

[11] FLEMINGS M C. Behavior of metal alloys in the semisolid state [J]. Metallurgical Transactions A, 1991, 22(5): 957−981.

[12] SEO P K, LEE S M, KANG C G. A new process proposal for continuous fabrication of rheological material by rotational barrel with stirring screw and its microstructural evaluation [J]. Journal of Materials Processing Technology, 2009, 209(1): 171−180.

[13] FAN Z, LIU G. Solidification behaviour of AZ91D alloy under intensive forced convection in the RDC process [J]. Acta Materialia, 2005, 53(16): 4345−4357.

[14] GUO Hong-min, YANG Xiang-jie, WANG Jia-xuan, HU Bin, ZHU Guang-lei. Effects of rheoforming on microstructures and mechanical properties of 7075 wrought aluminium alloy [J]. Transactions of Nonferrous Metals Society of China, 2010, 20: 355−360.

[15] FAN Z. Development of the rheo-diecasting process for magnesium alloys [J]. Materials Science and Engineering A, 2005, 413−414: 72−78.

[16] KAPRANOS P. Semisolid metal processing—A process looking for a market [J]. Solid State Phenomena, 2008, 141−143: 1−8.

[17] TANG H, WROBEL L C, FAN Z. Numerical analysis of the hydrodynamic behaviour of immiscible metallic alloys in twin-screw rheomixing process [J]. Materials & Design, 2006, 27: 1065−1075.

[18] GUO H M, YANG X J, HU B. Rheocasting of A356 alloy by low superheat pouring with a shearing field [J]. Acta Metallurgica Sinica, 2006, 19(5): 328−334.

[19] YANG Xiao-yong, MAO Wei-min, GAO Chong. Preparation of semisolid feedstock by serpentine pipe pouring [J]. The Chinese Journal of Nonferrous Metals, 2009, 19(5): 869−873. (in Chinese)

[20] WANNASIN J, MARTINEZ R A, FLEMINGS M C. Grain refinement of an aluminium alloy by introducing gas bubbles during solidification [J]. Scripta Materialia, 2006, 55(2): 115−118.

[21] WIESNER S, PAN Q Y, APELIAN D. Application of the continuous rheoconversion process to low temperature HPDC—Part II: Alloy development and validation [J]. Solid State Phenomena, 2006, 116−117: 64−67.

[22] YANG Liu-qing, KANG Yong-lin, ZHANG Fan, DING Rui-hua, LI Jiong. Rheo-diecasting of AZ91D magnesium by taper barrel rheomoulding process [J]. Transactions of Nonferrous Metals Society of China, 2010, 20(6): 966−972.

[23] ZHOU B, KANG Y L, ZHANG J, GAO J Z, ZHANG F. Forced convection rheomoulding process for semisolid slurry preparation and microstructure evolution of 7075 aluminum alloy [J]. Solid State Phenomena, 2013, 192−193: 422−427.

[24] ProCAST. User manual & technical reference [M]. USA: UES Software, Inc., 1997.

[25] TZIMAS E, ZAVALIANGOS A. Evaluation of volume fraction of solid in alloys formed by semisolid processing [J]. Journal of Materials Science, 2000, 35(21): 5319−5330.

[26] OHNO A. Solidification—Separation theory and its practical applications [M]. Berlin: Springger-Verlag, 1987: 83−118.

强制对流流变成形制备 7075 铝合金 半固态浆料及其数值模拟

周 冰 [1]，康永林 [1,2]，朱国明 [1]，郜俊震 [1]，祁明凡 [1]，张欢欢 [1]

1. 北京科技大学 材料科学与工程学院，北京 100083；
2. 北京科技大学 新金属材料国家重点实验室，北京 100083

摘　要：采用自主研发的强制对流流变装置，研究搅拌速度对 7075 铝合金半固态组织的影响规律。实验结果表明，随着搅拌速度的增加，半固态组织的晶粒尺寸减小，形状因子及粒子数增加。同时，对强制对流流变成形浆料制备过程进行数值模拟，研究熔体在筒体内的流动规律和搅拌速度对合金熔体温度场和固相率的影响。模拟结果表明，合金熔体在 FCR 筒体内存在复杂的对流运动，熔体对流极大地改变了合金熔体温度场和固相率的分布。增加对流强度有利于减小合金熔体的过冷度梯度和改善初生晶粒的分布。
关键词：7075 铝合金；强制对流流变成形；半固态浆料；制备；数值模拟

(Edited by Wei-ping CHEN)